WILEY | Hindawi

Research Article

Hydrocarbon Exploration Potential of the Jurassic Chaoshan Subbasin in Northern South China Sea: Evidence from the Latest Seismic and Outcrop Data

Kunsheng Qiang [1,2] **and Haipeng Li** [3,4,5]

[1]Southern Marine Science and Engineering Guangdong Laboratory (Guangzhou), 511458, China
[2]Guangzhou Marine Geological Survey, Guangzhou, Guangdong 511458, China
[3]School of Earth Sciences and Resources, China University of Geosciences, Beijing 100083, China
[4]Deep-Time Digital Earth Research Center of Excellence, Suzhou 215347, China
[5]Kunshan Industrial Technology Research Institute, Suzhou 215347, China

Correspondence should be addressed to Haipeng Li; haipeng.geo@gmail.com

For the first time, we have interpreted and delineated the distribution of Jurassic strata in the Chaoshan Subbasin, Pearl River Basin, in unprecedented detail using the newly collected seismic data (>17,000 km 2D seismic data and >580 km^2 3D seismic data). Four major reflection surfaces and three corresponding stratigraphic-structural layers were identified by analyzing seismic sections and borehole data from the LF35-1-1 well. Five distinct facies associations were identified within the stratigraphic-structural layers, including the shoreface, shallow marine, deep marine, deep-water fan, and mass-transport deposits. Based on outcrop observation, microscopic analysis, and geochemical evaluation, the Lower and Middle Jurassic deep marine mudstone has good source rock potential, and the Middle-Upper Jurassic deltaic sandstone and turbidite silty fine sandstone may be good reservoirs. Additional assessment of the study area's hydrocarbon potential has been conducted using the aromatic hydrocarbon content of seafloor sediments, and favorable exploration areas have been identified using BTEP (benzene, toluene, ethylbenzene, and xylene) content anomalies. Further simulations indicate that the Middle Jurassic hydrocarbon migration is primarily controlled by sand body distribution and faults. In summary, we propose that the most promising exploration targets should be structural (fault blocks), stratigraphic (sandstone lenses), and a combination of both.

1. Introduction

With the advancement of geological and geophysical research on the South China Sea and its surrounding areas, particularly the continental shelf in the northern part of the South China Sea, it is believed that the outcropped Late Triassic-Early Jurassic marine deposits on the South China Block extend into the sea, which indicates the possible presence of Late Triassic-Early Jurassic marine strata in the northern South China Sea [1–4].

Of particular interest is the Chaoshan Subbasin, which is part of the Pearl River Mouth Basin on the northern conti-

nental margin of the South China Sea (Figure 1). The Pearl River Mouth Basin is a subaqueous extension of the South China Block and is trending northeast. The Chaoshan Subbasin is connected to the Dongsha uplift on the northwest and southwest sides and the Southern uplift on the southeast. The area is about 39,000 km^2, and the Mesozoic sedimentary rocks have a maximum thickness of more than 5,000 meters (Figures 1 and 2(b)).

Based on the interpretation of seismic, gravity, geomagnetic, and regional geological data, many researchers (e.g., [1, 5]) concluded that the Chaoshan Subbasin is a representative Mesozoic residual basin on the northern margin of the
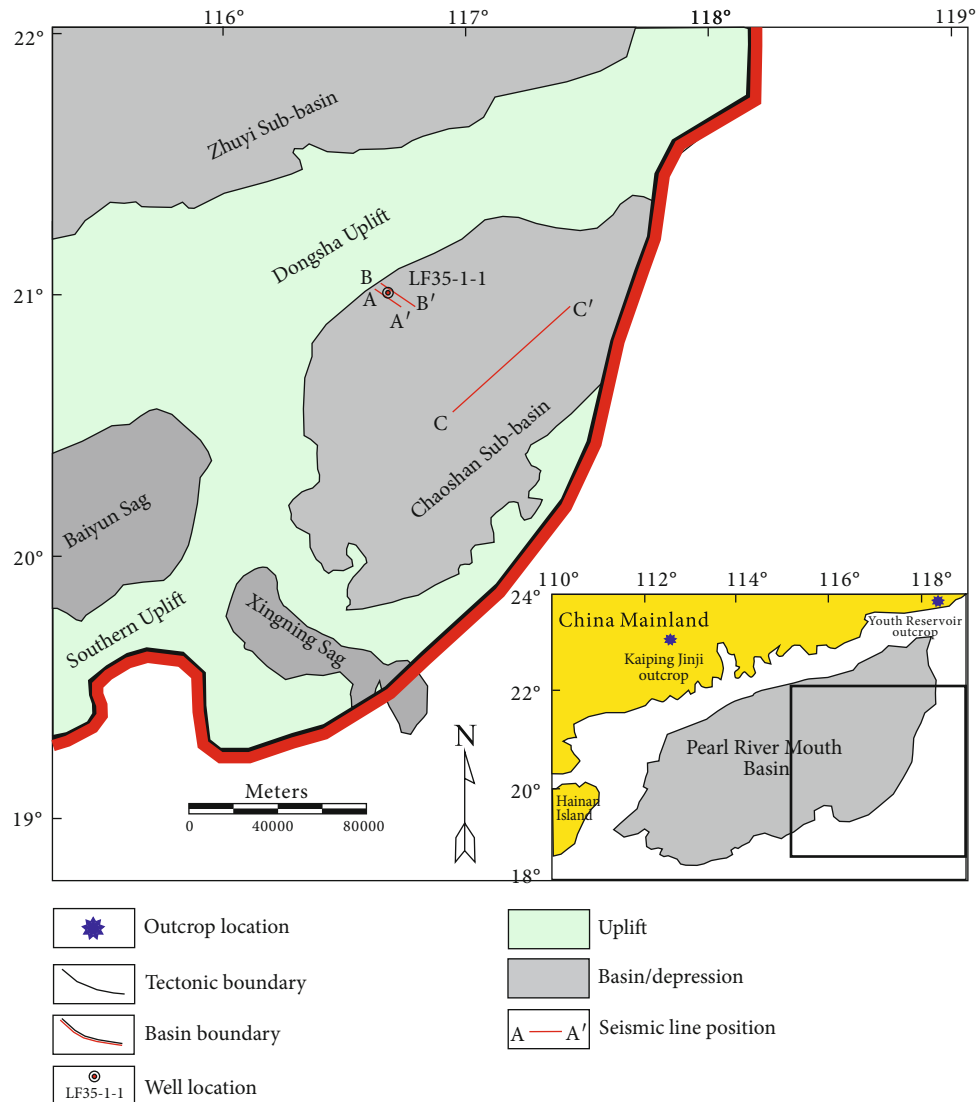
FIGURE 1: Simplified structural map of the Chaoshan Subbasin. The inset map shows the position of the Pearl River Mouth Basin and two outcrops.

South China Sea and the Pearl River Mouth Basin, and the Mesozoic strata are an important area for oil and gas exploration in the eastern part of the Pearl River Mouth Basin.

The LF35-1-1 well, drilled in September 2003 on the northern slope of the Chaoshan Subbasin, was the first exploration well in the eastern part of the Pearl River Mouth Basin to target the Mesozoic. The well confirmed the presence of Cretaceous continental deposits and Jurassic marine sediments in the Chaoshan Subbasin. The Jurassic marine sediments are suggested to have favorable petroleum geological conditions [6]. However, there was only fluorescence display in the drill cuttings and no evidence of industrial oil and gas flow. Nonetheless, this well provides critical information for understanding and studying the geological characteristics, petroleum geology, and the hydrocarbon-bearing prospect of the Chaoshan Subbasin.

One of the limiting factors for further research on the Mesozoic strata in this region is the lack of data. The primary objective of this study is to fill this gap with new data

and analyze the oil and gas exploration prospects of the Jurassic Chaoshan Subbasin based on the detailed Jurassic stratigraphic division, the latest regional geological survey outcrop data, and seismic data.

We will first briefly review the methods and the dataset used. We will then present a detailed analysis of the various components of the petroleum system in the Chaoshan Subbasin based on the new data. We conclude our study with suggested favorable plays, and we hope this study can serve as the foundation for the next step of oil and gas exploration in the Mesozoic in the northern South China Sea.

2. Methods, Samples, and Data

The Jurassic deposits are the key target of this study. We use recently collected seismic data, outcrop samples, and sea-bottom samples to study this interval's hydrocarbon potential systematically.
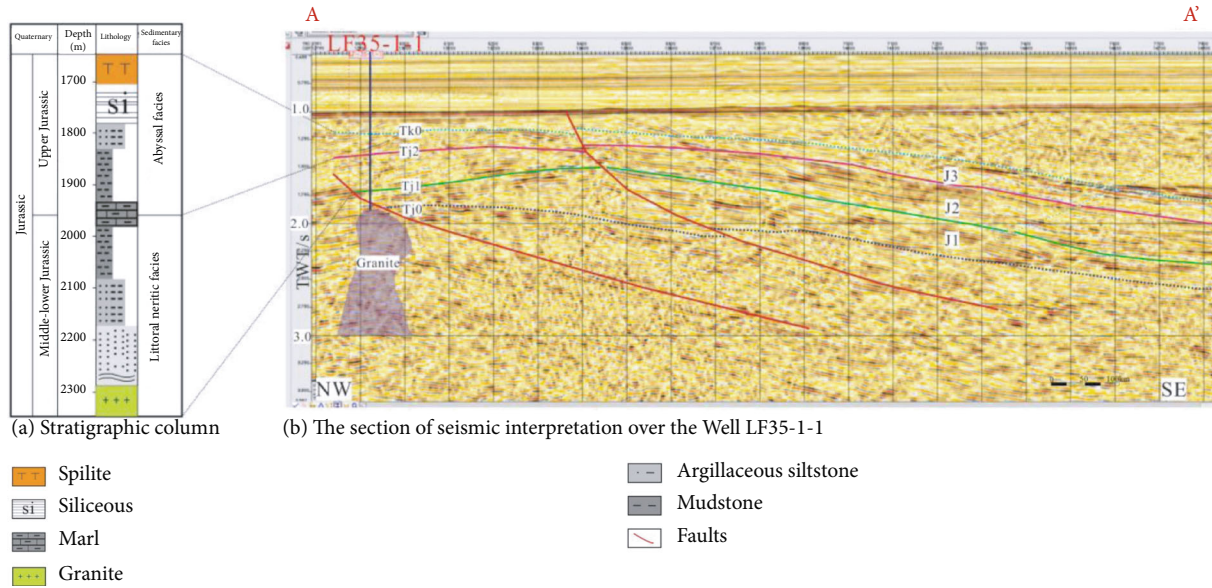
Figure 2: (a) Stratigraphic column of LF35-1-1 well; (b) interpreted seismic section across the LF35-1-1 well (see Figure 1 for locations of profiles).

The seismic data used in this study are mainly from the 1,890 km of 2D seismic data acquired by the Guangzhou Marine Geological Survey's survey ship "TANBAO HAO" in 2017 and the 580 km^2 of 3D seismic data volume. The seismic data interpretation is made using Schlumberger's Geoframe (2012 version).

The outcrop samples were collected by the Guangzhou Marine Geological Survey from November 30 to December 7, 2017, in the eastern and western Guangdong regions. To meet the needs of source rock and reservoir research, a total of four outcrop sections were surveyed, 109 samples were collected, and 776 photos were taken.

Sediment samples from deep water were collected by the "Ocean No. 4" geological survey vessel of the Marine Geological Survey of Guangzhou. The vessel collected sediment samples via gravity and piston sampling at a depth of 5 m to minimize the effect of bioturbation.

The aromatic hydrocarbon test equipment is the GC2010 PLUS gas chromatography-mass spectrometer (SHIMADZU Japan Tsushima Corporation), Agilent 5975 mass spectrometer (Agilent Technologies, USA), and UNITY100 automatic thermal desorber for aromatic hydrocarbons (Markers Technology, UK).

For the pyrolysis of source rock samples, the heat balance temperature was 320°C, the transfer line temperature was 300°C, the trap temperature was 300°C, and the low-temperature adsorption was -25°C. The heating rate was 40°C/s, and the column flow rate was 1.0 mL/min. The column was DB-5MS, the column length was 60 m, the wall thickness was 0.5 μm, and the column diameter was 0.32 mm. The carrier gas is pure helium.

The gas chromatographic temperature rising conditions were 50°C for 2 min, then steadily rising to 320°C at a rate of 11°C/min; the temperature was then held constant for 15 min. The mass spectrometer inlet temperature is 300°C, the ion source temperature is 250°C, and the surface temperature is 250°C. The full scan data acquisition mode has a scan range of 35~350 m/z, with a full scan time of 0.2 s and a scan time interval of 0.05 s.

3. Results and Discussion

3.1. Stratigraphic Framework. Four major Jurassic reflection surfaces and three corresponding stratigraphic-structural layers can be clearly identified through analysis of seismic sections and comparison with borehole data of the LF35-1-1 well in the Chaoshan Subbasin (Figure 2). The four reflection surfaces are Tj0 (the Lower Jurassic bottom surface), Tj1 (the Middle Jurassic bottom surface), Tj2 (the Upper Jurassic bottom surface), and Tk0 (the Upper Jurassic top surface). Tj0-Tj1 corresponds to the Lower Jurassic structural layer (J1), Tj1-Tj2 corresponds to the Middle Jurassic structural layer (J2), and Tj2-Tk0 corresponds to the Upper Jurassic structural layer (J3).

The top of the J1 layer is a regional, near-parallel surface that separates high-amplitude, low-frequency, and continuous reflections above from the medium-amplitude discontinuous reflections below. The bottom of the J1 layer coincides with the base of the Jurassic System and consists of two parallel high-amplitude reflections. Internally, the J1 layer is characterized by parallel to subparallel seismic reflections with medium frequency and high amplitude (Figure 2(b)). The sediments in this layer are interpreted to be shallow marine deposits. The lithology in the lower part of this layer is mainly metamorphosed sandstone and granite, showing igneous rock intrusion (Figure 2(a)).

In addition to the seismic data, we conducted a field survey of two Early Jurassic outcrops in the Guangdong province (Figure 1). The first outcrop is near the Youth Reservoir of Haifeng County. The Jurassic strata here have a large thickness and good exposure. The three formations from older to younger are the Shanglongshui Formation
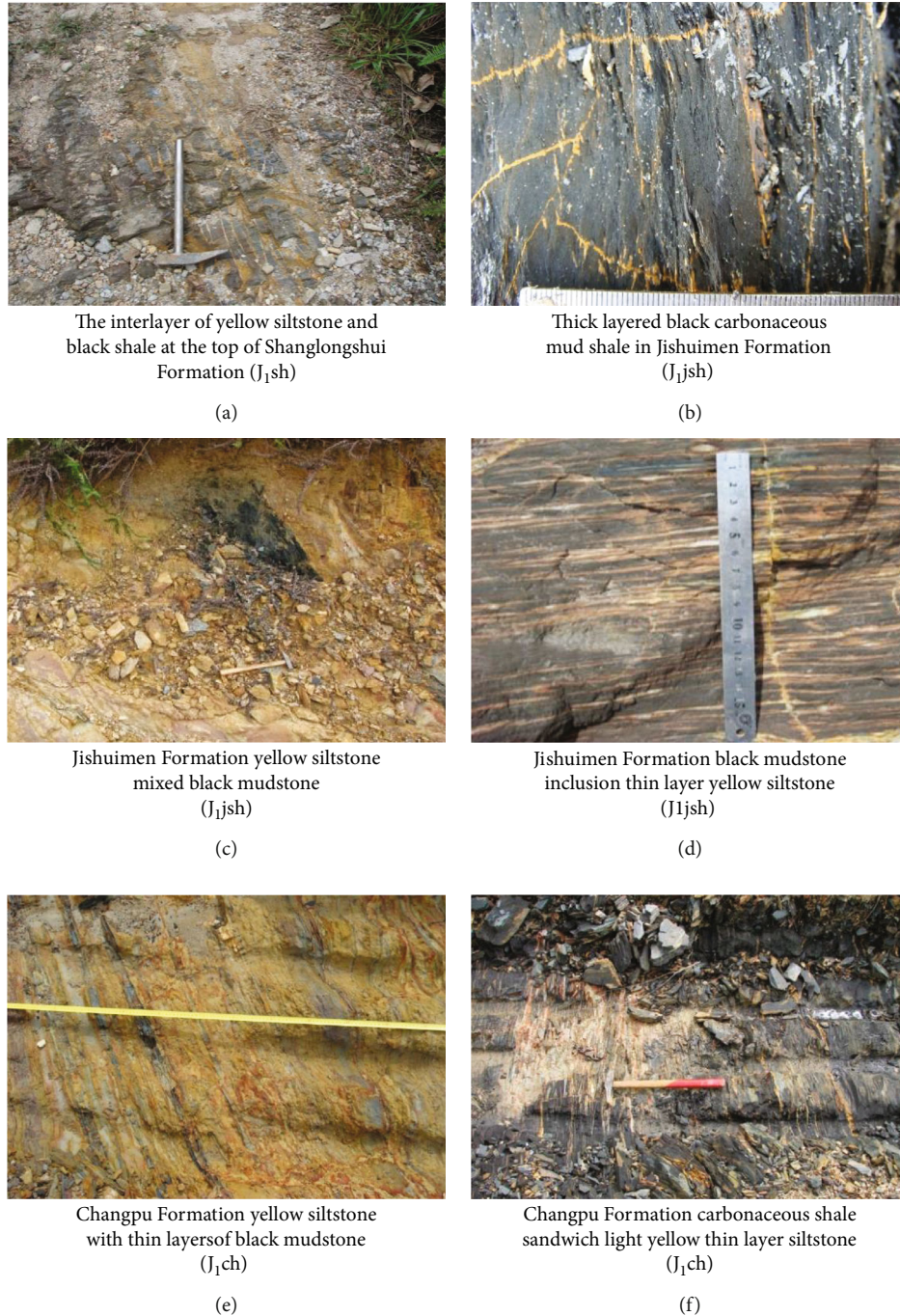
The interlayer of yellow siltstone and
black shale at the top of Shanglongshui
Formation (J_1sh)

(a)

Thick layered black carbonaceous
mud shale in Jishuimen Formation
(J_1jsh)

(b)

Jishuimen Formation yellow siltstone
mixed black mudstone
(J_1jsh)

(c)

Jishuimen Formation black mudstone
inclusion thin layer yellow siltstone
(J1jsh)

(d)

Changpu Formation yellow siltstone
with thin layersof black mudstone
(J_1ch)

(e)

Changpu Formation carbonaceous shale
sandwich light yellow thin layer siltstone
(J_1ch)

(f)

Figure 3: Photographs of typical source rocks of the Haifeng Youth Reservoir section.

(J_1sh), Changpu Formation (J_1ch), and Jishuimen Formation (J_1jsh), respectively. The lithology of the Shanglongshui Formation (J_1sh) is mainly shale, with yellow siltstone and black shale interbeds at the top (Figure 3(a)); the Jishuimen Formation (J_1jsh) is characterized by gray-black thick bedded carbonaceous shale, black mudstone with thin layers of yellow siltstone, and yellow siltstone with black mudstone interbeds (Figures 3(b)–3(d)). The primary lithologies of the Changpu Formation (J_1ch) include mudstone and a set of yellow siltstones with thin layers of black mudstone, which transition into carbonaceous shales with light yellow

thin layers of siltstone (Figures 3(e) and 3(f)), and black mudstones and carbonaceous shale with a thickness of 2 m~10 m. These observations are consistent with the seismic facies of the J1 layer.

The second outcrop is near a mine on the north side of Jinji Town, Kaiping City. Stratigraphically, the Early Jurassic Jinji Formation (J_1jj) at this outcrop can be correlated with the other three formations in Haifeng County. At the bottom, the Jinji Formation is characterized by gray and brown medium-grained quartz sandstone with thin shale layers (Figures 4(a)–4(d)) that contain bivalve fossils, which
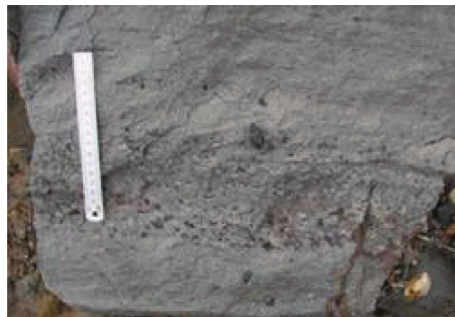
The outcrop of Jinji Formation is dominated by gray and yellow sandstone

(a)
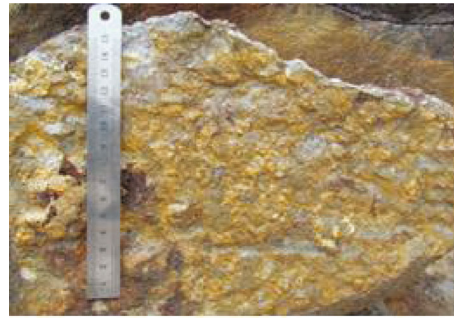
The coarse gray quartz sandstone near the bottom of the Jinji Formation

(b)

The pebbly sandstone at the bottom of the Jinji Formation

(c)

The middle and lower parts of the Jinji Formation are fine quartz sandstones

(d)

The ammonite of the Jinji Formation

(e)

The upper gray fine grain quartz sandstone of the Jinji Formation

(f)

FIGURE 4: Typical lithology of the Jurassic Jinji Formation (J_1jj) in Kaiping Jinji section.

indicate a shallow marine environment. Upward, the grain size decreases, and the lithology is dominated by fine-grained quartz sandstone and sandy shale, with intercalations of gray-purple siltstone and argillaceous siltstone that has ammonite fossils (Figure 4(e)), indicating a relatively deeper environment. Near the top, the formation is mainly gray fine quartz sandstone and siltstone (Figure 4(f)). Overall, the Jinji Formation fines upward, and the coarser quartz sandstone at the bottom is potentially a good reservoir. The interpreted shallow marine environment is also consistent with the seismic facies interpretation.

The top of the J2 layer is a disconformity characterized by wavy variable-amplitude reflection, which truncates the underlying strata. The early faults usually end near this sur-

face, indicating that large-scale tectonic movements occurred in the Chaoshan Subbasin during this period, which had a large impact on the structural pattern of the entire Chaoshan Subbasin. The internal subparallel reflections have medium frequency, strong amplitude, and good continuity (Figure 2(b)).

The top of the J3 layer is an unconformity surface, and the bottom surface is characterized by toplap and truncation, with wavy variable-amplitude reflection. The internal reflections have medium to high frequency, suggesting relatively continuous deposition in this period (Figure 2(b)). The lithology is mainly mudstone, with mudstone and marl near the bottom and siliceous rock at the top (Figure 2(a)), indicating mainly deep-water sedimentation.
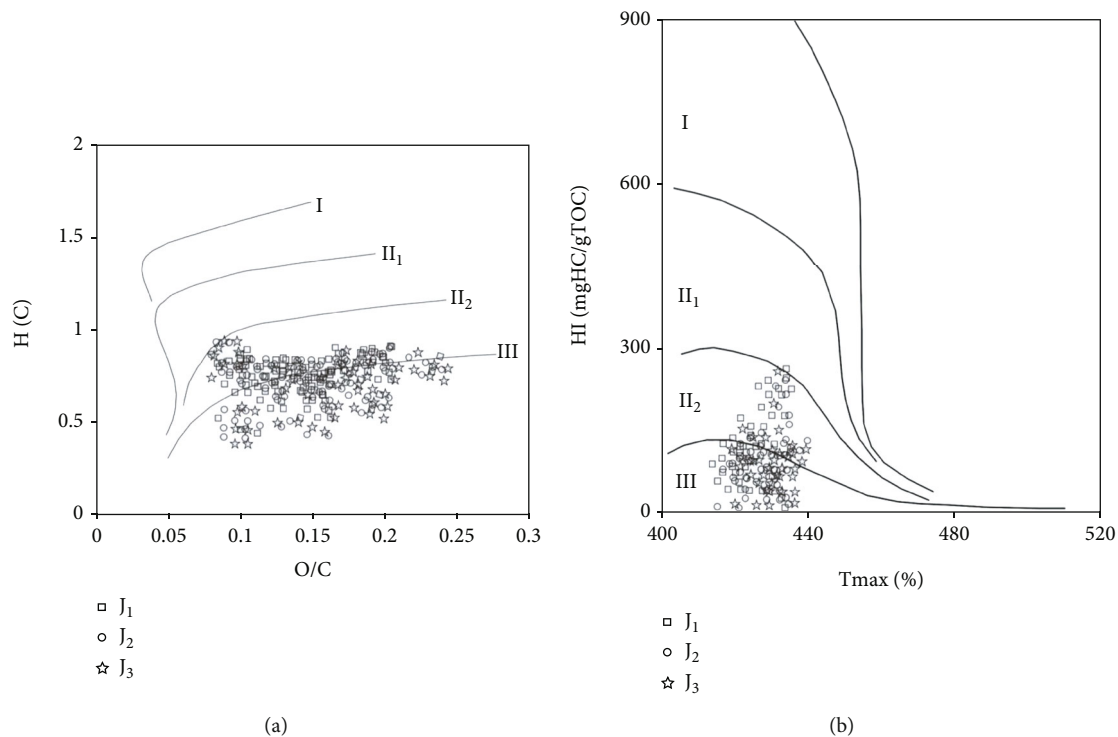
(a)

(b)

FIGURE 5: The kerogen types of the Jurassic source rocks in the Chaoshan Subbasin.

TABLE 1: Geochemical characteristics of J3, J2, and J1 source rocks in Chaoshan Subbasin.

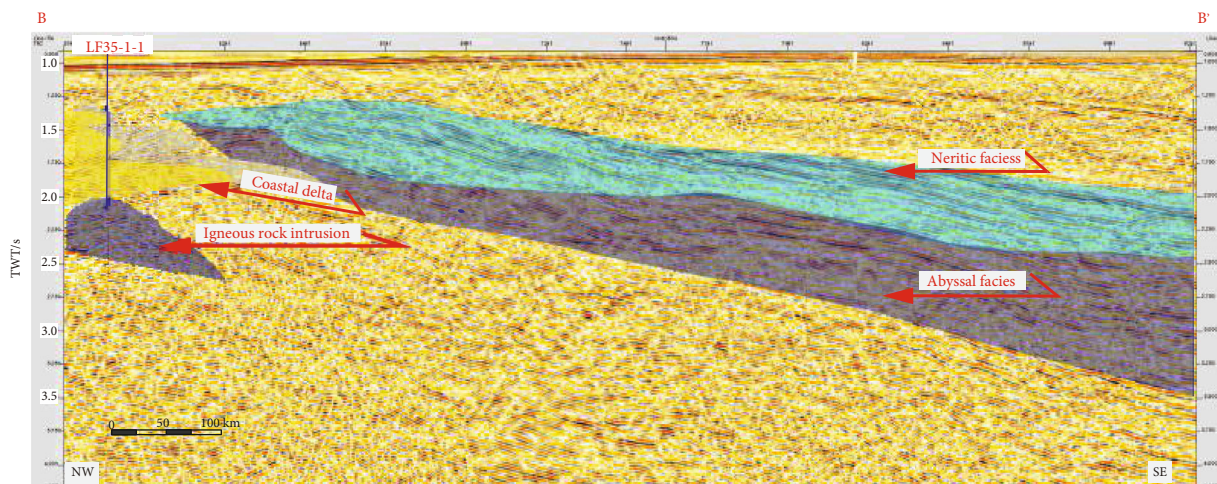| Horizon	$S_1 + S_2$ (mg/g)	T_{max} (mg/g)	TOC (mg/g)	HI (mg/g)	
J3	3.77 (33)	425 (33)	0.87 (33)	239 (33)	A (B)
	0.4~5.46	431~489	0.18~2.15	100~427	C-D
J2	5.76 (26)	446 (26)	2.37 (26)	257 (26)	A: Ave.
	0.2~26.77	426~496	1~4.87	19~499	B: Num.
J1	5.77 (21)	455 (21)	1.85 (21)	311 (21)	C: Min.
	0.25~9.6	428~478	0.49~6.49	0.11~469	D: Max.

FIGURE 6: The characteristic profile of seismic and sedimentary facies (see Figure 1 for locations of the profile).

J1ch, –N, plane-polarized light, 4×10, 0.8 mm

(a)

J1ch, +N, cross-polarized light, 4×10, 0.8 mm

(b)

J1sh,-N, plane-polarized light, 4×4, 2mm

(c)

J1sh, +N, cross-polarized light, 4×4, 2mm

(d)

J1jsh, -N, plane-polarized light, 4×10, 0.8mm

(e)

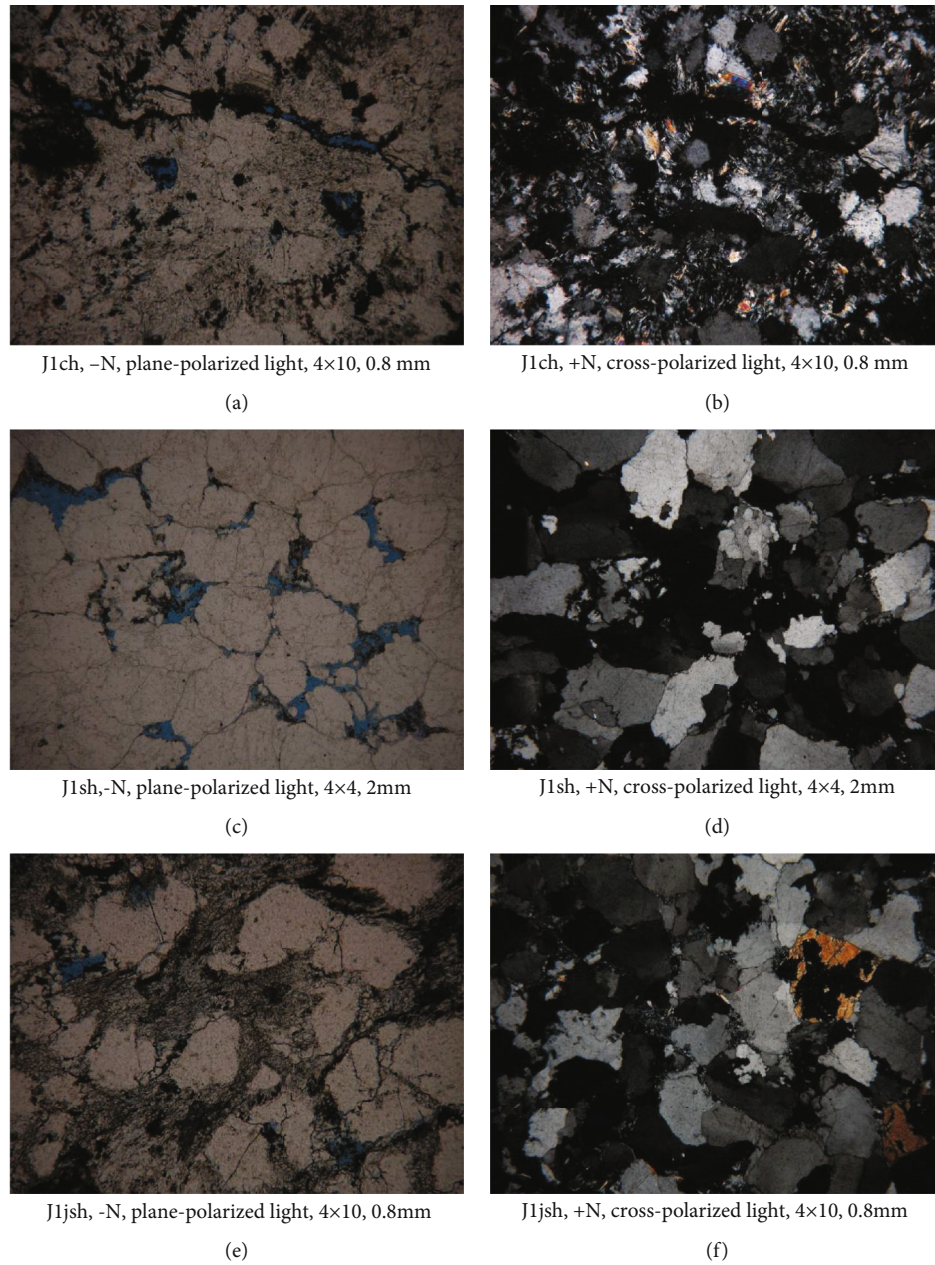J1jsh, +N, cross-polarized light, 4×10, 0.8mm

(f)

FIGURE 7: Identification of pore types in the Early Jurassic sandstone samples from the Kaiping Jinji section.

3.2. Source Rocks. Source rock conditions are fundamental for the formation of oil and gas. The quality of source rocks directly determines the hydrocarbon generation potential [7–10]. Given the drilling data scarcity in the Chaoshan Sub-basin, geochemical evaluation of the source rocks has been done for the cores of the Tainan Basin, the Liletan Basin, and the Mindoro Island of the Philippines and the outcrop area of the South China Block [11]. For instance, Hao et al. [12] suggest that the TOC of the outcropping Mesozoic mudstones in the Guangdong region is high and rich in regular steranes, with the C27 sterane content accounting for 41%~60%, indicating that the source rock has reached maturity. The TOC of the Upper Triassic source rock is 0.35% to 6.75%, the R_o value is 1.1% to 1.59%, and the source rock is type III. Similarly, the Lower Jurassic source rock is also type III, with a TOC value of 0.5% to 2.0% and R_o value of 2.69% to 3.75%, which has reached maturity. According to et al. [13], the Upper Cretaceous Yetang Formation mudstone in the eastern Guangdong region is rich in regular steranes, with a content of 41%-60%, indicating that the source of the organic matter is mainly plankton (Figure 5).

The LF35-1-1 well reveals that the upper part of the Middle-Upper Jurassic is gray-black layered mudstone, argillaceous siltstone, and siliceous rock with a small amount of mudstone; the lower part is gray-black layered mudstone and argillaceous siltstone with sandstone and limestone interbeds, with the mudstone being rich in organic matter. Geochemical analysis shows that there exist three primary
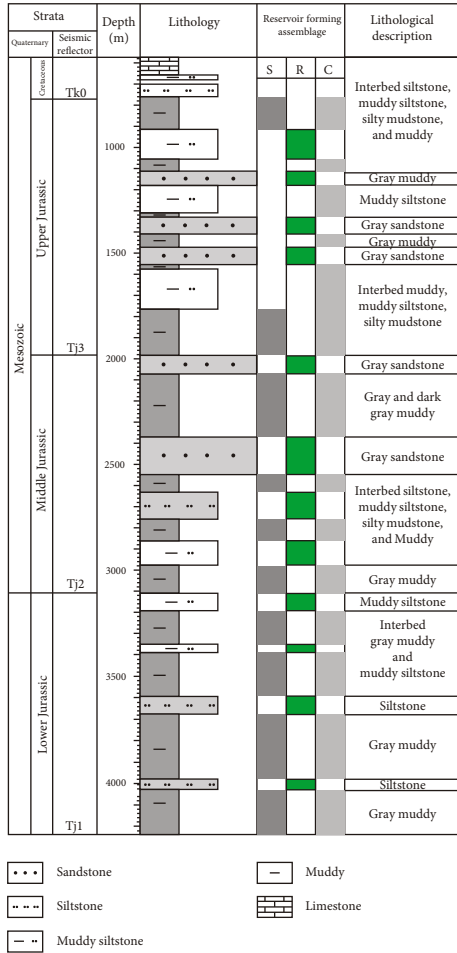
FIGURE 8: Combination of Jurassic reservoirs and cap rocks in Chaoshan Subbasin.

source rocks, of which the Middle Jurassic and Lower Jurassic are the best, and the Upper Jurassic is the secondary source rock.

Based on the statistical analysis of 122 source rock samples from the LF35-1-1 well, the Lower Jurassic source rocks are mainly found in the depth range of 2,150 m~2,400 m, with a cumulative thickness of 185.25 m. The total organic carbon content (TOC) is between 0.49 and 6.49%, with a mean of 1.85%, which indicates [14] that the Lower Jurassic source rock has fair to good richness. The hydrocarbon generating potential ($S_1 + S_2$) of the samples from pyrolysis is 0.25~9.6 mg/g, with the mean being 5.77 mg/g. T_{max} for S_2 is between 428 and 478°C, with a mean of 455°C. The pyrolysis hydrogen index ranges between 0.11 and 469 mg HC/g TOC, with an average value of 311 mg HC/g TOC. The kerogen H/C atomic ratio is between 0.5 and 0.95, and the O/C atomic ratio is between 0.07 and 0.24; this suggests that the kerogen is mainly type III on a van Krevelen diagram (Table 1; Figure 5). Together, the kerogen type and T_{max} indicate that the source rock is the oil generation zone [15].

The Middle Jurassic source rocks are found primarily in the depth range of 1,870 m~2,150 m, with a cumulative thickness of 135.75 m. The TOC is between 1.00 and

4.87%, and the average value is 2.37%. It is a fair to very good source rock in terms of organic matter richness. $S_1 + S_2$ is 0.2~26.77 mg HC/g rock, and the average is 5.76 mg HC/g rock. T_{max} for S_2 is between 426 and 496°C, with a mean of 446°C. The hydrogen index ranges between 19 and 499 mg HC/g TOC, with an average of 257 mg HC/g TOC. The kerogen H/C atomic ratio is between 0.5 and 0.98, and the O/C atomic ratio is between 0.075 and 0.25; this suggests that kerogen is mainly type III on a van Krevelen diagram (Table 1; Figure 5). The kerogen type and T_{max} also indicate medium maturity of the source rock in the oil generation zone [15]. Overall, the Middle and Lower Jurassic source rocks have relatively deep burial depths and large thicknesses.

The Upper Jurassic source rocks are mainly in the range of 1,720 m~1,860 m, and the cumulative thickness is 80.5 m. The TOC is between 0.18% and 2.15%, and the average value is 0.87%. It is a poor-fair source rock in terms of organic matter richness. $S_1 + S_2$ is 0.4~5.46 mg HC/g rock, the average content being 3.77 mg HC/g rock. T_{max} for S_2 is between 431 and 489°C, with a mean of 445°C indicative of medium maturity. The hydrogen index is between 100 and 427 mg HC/g TOC, with an average of 239 mg HC/g TOC. The kerogen H/C atomic ratio is between 0.3 and 0.75, and the O/C atomic ratio is between 0.06 and 0.29; this suggests that the kerogen is mainly type III on a van Krevelen diagram (Table 1; Figure 5). In comparison, the Upper Jurassic source rocks have shallower burial depth and lower maturity.

3.3. Reservoir. Mesozoic strata are well developed in the Chaoshan Subbasin. Previous research has identified the Middle to Upper Jurassic shallow marine and deltaic sandstones and the deep-water fan sandstones as the main reservoir, whereas the Upper Cretaceous lacustrine sandstone is a potential reservoir [5, 16–20].

Provenance studies suggest that the sediments are mainly from the north and northwest. The primary sedimentary facies include delta and shoreface facies, shallow and deep marine facies, deep-water fans, and mass-transport deposits. The delta front facies displays a characteristic mounded shape and continuous strong reflections on the seismic section; the prodelta facies consists of continuous weak reflections that migrate progressively into the basin, exhibiting unstable lateral sand body distribution and lithological changes. The shallow marine facies has medium frequency, low amplitude, and continuous reflections, indicating lateral lithological stability. The deep marine facies is characterized by wavy, parallel reflections, indicating a low energy state of the water body and stable, uniform deposition. The turbidite facies displays irregular and discontinuous reflections, suggesting lateral variability in deposition (Figure 6).

The analysis of well LF35-1-1 and seismic data reveals the presence of two reservoirs in the Mesozoic of the Chaoshan Subbasin: a Cretaceous fluvial-lacustrine sand body and the Middle-Upper Jurassic sandstones formed in shallow marine, slope, and basin-bottom fan and the transgression systems. Among these, the sandstone of the Middle-Upper Jurassic stands out as the primary reservoir.

TABLE 2: Sediment aromatic characteristic statistics of Chaoshan Subbasin.

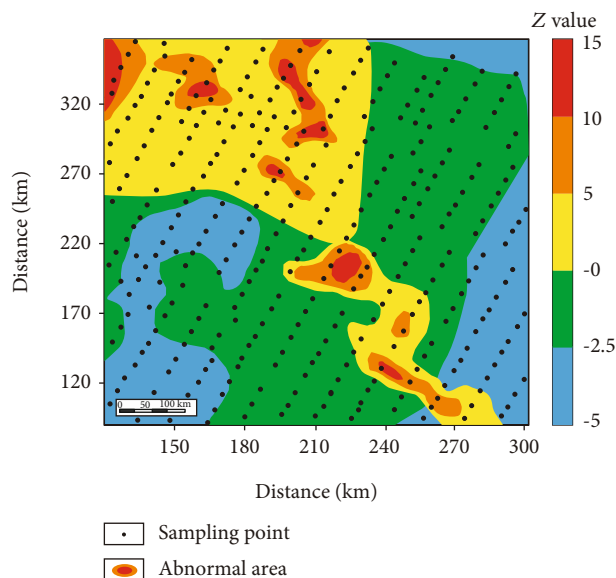| Eigenvalues	Benzene (%)	Toluene (%)	Ethylbenzene (%)	Paraxylene (%)	o-Xylene (%)
Number	366	366	366	366	366
Max.	82476.5	16598.5	9320.5	16955	34231
Min.	3578	650	188	10	185
Ave.	15666	3780	1450	3105	8677

FIGURE 9: Plan view of anomalous aromatics in the Chaoshan Subbasin.

This sandstone has a total thickness of 120 m and a maximum single-layer thickness of 40 m. However, its porosity is low. Seismic sections of these strata display a set of low-frequency, high-continuity, and strong amplitude reflections, indicating the presence of continuous and stable marine sand bodies over a wide range.

We also sampled the onshore outcrops for thin section analysis. The primary lithology of the Jurassic Changpu Formation (J_1ch) in Haifeng County is fine-grained quartz sandstone with visible fractures and dissolution porosity filled with slightly metamorphized illite (Figures 7(a) and 7(b)). The primary lithology of the Shanglongshui Formation (J_1sh) reservoir in the Upper Jurassic is medium-coarse quartz sandstone with intergranular dissolved pores and a surface porosity of 6% (Figures 7(c) and 7(d)). The primary lithology of the Jurassic Jishuimen Formation (J_1jsh) reservoir is medium-coarse quartz sandstone dominated by single-crystal quartz and polycrystalline quartz, and illite is the primary matrix. The reservoir has an average surface porosity of 2%, which consists mainly of intergranular pores (Figures 7(e) and 7(f)).

3.4. Reservoir and Cap Rock Combination.

The interbedding of sandstone and mudstone is ubiquitous in the Chaoshan Subbasin. The Jurassic marine shales are not only good hydrocarbon source rocks but also excellent regional cap rocks. The shallow marine and abyssal shales widely distrib-uted throughout the region during the mid-late Jurassic and thereafter are good cap rocks, with abyssal shale having a relatively homogeneous composition and better sealing ability.

In the study area, the Jurassic deltaic, shallow marine and turbidite sandstones, and the shallow marine shales make up the primary reservoir-cap rock combination, which is the main exploration target in Chaoshan Subbasin. The Lower Jurassic black carbonaceous shale has good hydrocarbon generation conditions and is a potential source rock. The gray sandy shale may have less favorable hydrocarbon generation conditions. However, due to its large thickness, the sandy shale has some sealing capability and may be a good cap rock (Figure 8).

3.5. Surface Geochemical Exploration in Seabed Sediments.

It has long been recognized that hydrocarbons trapped at depth will leak to the surface in varying but detectable amounts [21]. Geochemical anomalies formed by hydrocarbon leakage may be detected in surface sediments to predict the presence of hydrocarbon reservoirs [22–26]. One of the most salient geochemical features of coal-type gas fields is the high content of benzene and toluene in gas. The gas reservoirs discovered in the shallow waters of the Pearl River Mouth Basin and Qiongdongnan Basin in the South China Sea are characterized by high levels of benzene and toluene, in good correlation with the source rocks [27].

Due to the high content of aromatics in natural gas in the study area, sampling and detecting trace amounts of aromatics in seabed sediments may be an efficient and economical way to narrow down the target areas. Seabed sediments were sampled from June to August 2017, followed by the geochemical analysis of benzene, toluene, ethylbenzene, and xylene (p-, o-, and m-xylene) (BTEP). The statistical results show a significant positive correlation between benzene, toluene, ethylbenzene, and xylene (p-, o-, and m-xylene) in marine sediments (Table 2).

According to the analysis of each index, the sum of the standardized values of the aromatics (Z value) is consistent with the contribution of anomaly weights, based on which a comprehensive anomaly map is drawn (Figure 9). The anomalies have an overall trend of southeast-northwest and extend westward to the Dongsha uplift area. The distribution of the anomalies corresponds with the structural units, providing an important reference for subsequent well drilling. High-value aromatic anomaly areas are in patchy and banded shapes and are found mainly in the northwest slope area and the central uplift of the Chaoshan Subbasin at water depths of 1,000~1,500 m. The seismic line AB crosses these areas, and the combined results suggest that the northwest slope and the central uplift are the preferred
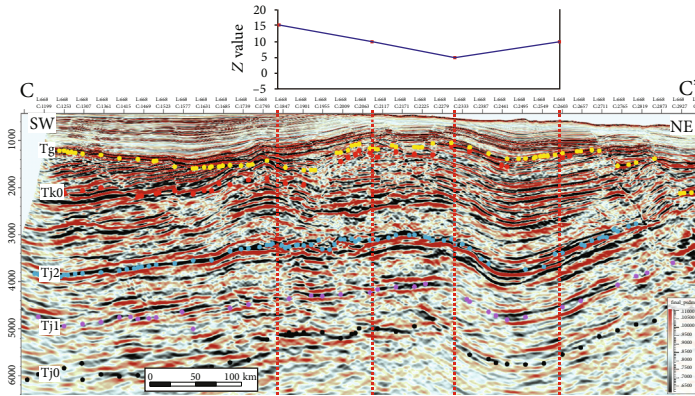
FIGURE 10: The comparison between the Chaoshan Subbasin seismic section and the BTEX section (see Figure 1 for locations of the profiles).
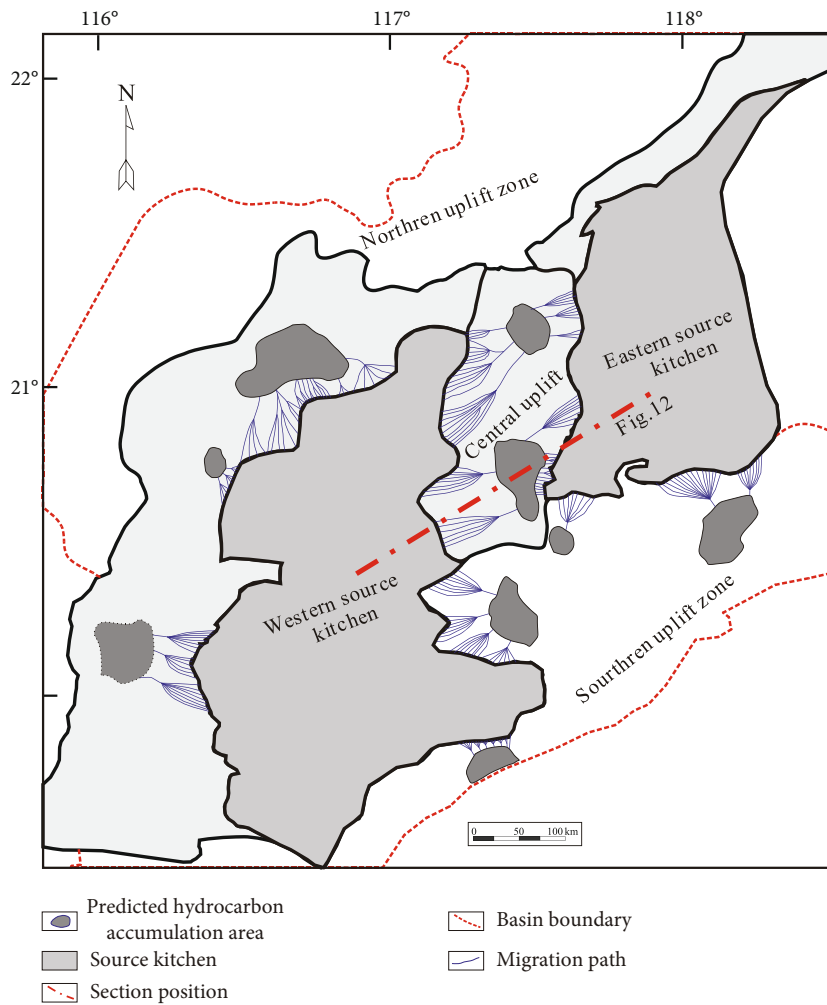

FIGURE 11: Schematic diagram of hydrocarbon migration and accumulation in Middle Jurassic in Chaoshan Subbasin.

drilling targets. There is no apparent aromatic occurrence in the southern uplift (Figure 10).

3.6. Hydrocarbon Migration and Accumulation Modeling. The current geothermal field gradient of the Pearl River Mouth Basin is 26.2~50.6°C/km, with an average of 33.1°C/ km. The highest value of 49°C/km is found in Dongsha uplift, and the lowest value of 28.1°C/km is found in Xijiang Sag [28]. The paleotemperature gradient of well LF35-1-1 was used to reconstruct the thermal history. In the late Mesozoic, the well experienced the highest heat flux of $107 \, \text{mW/m}^2$, with a paleotemperature gradient of 42°C/km.
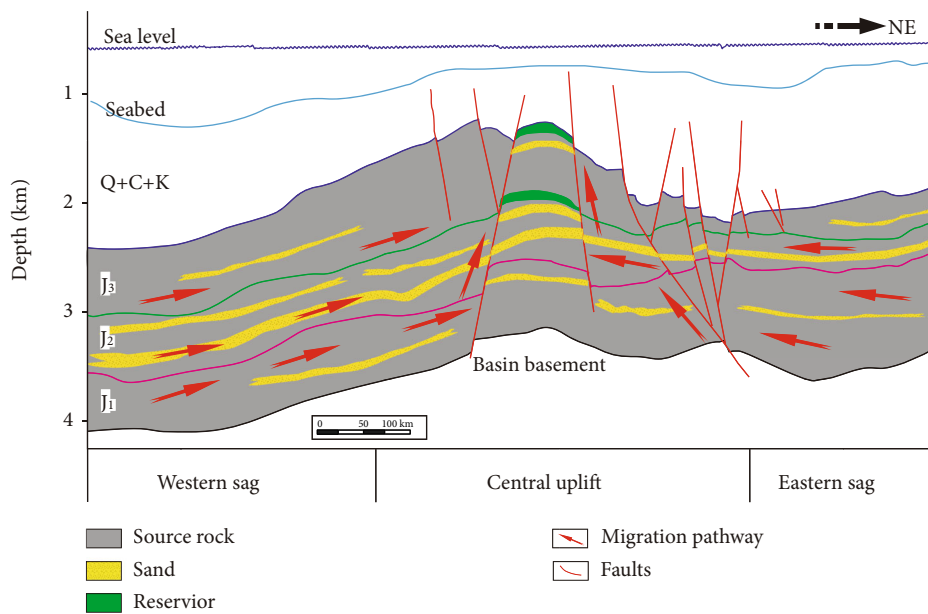
FIGURE 12: Hydrocarbon accumulation pattern in Chaoshan Subbasin (see Figure 11 for locations of profiles).

The R_o value of well LF35-1-1 generally increases linearly from top to bottom, and the R_o value at 1700 m has a sudden increase, which may be related to igneous rock intrusion in this area. Below 1,700 m, the R_o value is greater than 2.0%. At about 2,400 m, the R_o value reaches 3.0%, and the source rock has entered the late stage of maturity [6].

The PATHWAYS™ model [29] was used for 3D hydrocarbon migration path simulation (Figure 11). Lower and Middle Jurassic TOC is greater than 1.5%, and thermal maturity R_o is larger than 2.5%, which can be identified as a source kitchen. The western sag (source kitchen) with deeper burial is the main hydrocarbon sag, and the eastern sag (source kitchen), which is buried deeper, is the secondary. Simulation results show that the middle sandstone layer of the Middle Jurassic is the migration channel, and the mudstone at the top of the Middle Jurassic is the cap rock. The hydrocarbon migration direction derived from aromatic component leakage in seabed sediments correlates well with the simulated hydrocarbon migration path.

The oil sources of predicted Upper and Middle Jurassic reservoirs are derived from Lower Jurassic and Middle Jurassic source rocks in the western sag and eastern sag. Based on our model, oil and gas are mainly stored in the Upper Jurassic reservoir and some in the Middle Jurassic reservoir. The overlying Upper and Middle Jurassic marine mudstones have a thickness of hundreds of meters, showing excellent seal capacity. There are mainly two types of faults: a NE-trending sag-controlling fault, mainly the No. 1 and No. 2 faults, and the extensional near-east-west fault. In addition to the strong activity of the sag-controlling fault in the early stage of basin formation, these faults had two more periods of activity: Late Jurassic-Cretaceous and Paleogene. The faults were more active during the Paleogene, and the near-east-west-trending fault was formed in this period. The trap also formed mainly during this period as the source

rock reached maturity. Afterward, the source rock began to generate a large amount of hydrocarbon. The large-scale accumulation in the area took place from 23 Ma to the present. During this time, the traps were in place, and the structures were stable. Therefore, oil and gas migration and accumulation in this area are mainly controlled by a composite system consisting of sand bodies and faults rather than fault activity (Figure 12).

4. Conclusions

Based on the newly acquired seismic data, the drilling data, outcrop observation, microscopic analysis, and geochemical evaluation of outcrop and seabed sediment samples, the following conclusions can be drawn:

(1) The Chaoshan Subbasin is a depression with great hydrocarbon potential. The Mesozoic deep marine mudstone has a large thickness, serving as either source rocks or regional cap rocks. The main source rocks are found in the Lower and Middle Jurassic, with great burial depth, large thickness, and high thermal maturity. The interbedded sandstone and mudstone of the Middle and Upper Jurassic are the main reservoirs

(2) The Chaoshan Subbasin experienced a complete depositional cycle from the late Jurassic to the early Cretaceous, starting with shallow water sedimentation systems and then transitioning to deeper water before finally becoming a terrestrial environment. Based on seismic and sedimentary facies analysis, five distinct facies associations, including that of the shoreface, the shallow marine, the deep marine, the deep-water fan, and mass-transport deposits, were identified

(3) The standardized values (Z values) of the aromatic hydrocarbon index indicate that high-value aromatic anomalies are in patchy and banded shapes; the anomalies are located mainly in the northwest slope area and the central uplift of the Chaoshan Subbasin, which have structural traps and are the preferred drilling targets

(4) Oil and gas migration and accumulation in this area are mainly controlled by a composite system consisting of sand bodies and faults, and structural and structural-stratigraphic accumulations, including the small fault block and sand body lenses, are the key targets

Data Availability

Data not available due to commercial restrictions.

Conflicts of Interest

The authors declare that they have no conflicts of interest.

Authors' Contributions

Kunsheng Qiang contributed to the conceptualization, study design, methodology, investigation, data analysis, funding acquisition, and writing of the original draft. Haipeng Li contributed to the research question, data analysis, review, and editing and assisted with manuscript preparation and revision.

Funding

Acknowledgments

References

[1] D. Jiuchun and M. Huifen, "Seismic facies and sedimentary facies study of Mesozoic in Chaoshan sag," *Resources and Industries*, vol. 14, no. 1, pp. 100–105, 2012.

[2] Y. Shaokun, L. Heming, and H. Hujun, "Oil and gas exploration prospect of mesozoic in the eastern part of pearl river mouth basin," *Acta Petrolei Sinica*, vol. 23, no. 5, pp. 28–33, 2002.

[3] W. Zhong Guangjian, L. Z. Nengyou, Y. Yongjian, and Y. Hai, "Characteristics of faults on the northeastern continental slope of the South China Sea and their controls on basin evolution," *Geology in China*, vol. 35, no. 3, pp. 456–462, 2008.

[4] D. Zhou, Z. Sun, and H. Chen, "Tectonic features of world's major deep-water oil/gas fields and their enlightenment to deep-water exploration in Northern South China Sea," *Advances in Earth Science*, vol. 22, no. 6, pp. 561–572, 2007.

[5] C. Jie, "Geophysical characteristics of the Chaoshan sub-basin and its hydrocarbon exploration potential," *Progress in Geophysics*, vol. 22, pp. 147–155, 2007.

[6] S. C. Yang, Z. G. Tong, Q. He, and J. R. Hao, "Mesozoic hydrocarbon generation history and igneous intrusion impacts in Chaoshan depression, South China Sea: a case of LF35-1-1 well," *China Offshore Oil and Gas*, vol. 20, no. 3, pp. 152–156, 2008.

[7] L. Jinpingl, W. Liaoliang, W. Gaiyun, L. Zhenhu, D. Minla, and J. Xiaolingl, "Analyzing characteristics of Mesozoic hydrocarbon source rocks in the Eastern depression, North Yellow Sea basin," *China Offshore Oil and Gas*, vol. 25, no. 4, 2013.

[8] W. Li, Z. Zhang, Y. Li, and N. Fu, "The effect of river-delta system on the formation of the source rocks in the Baiyun Sag, Pearl River Mouth Basin," *Marine and Petroleum Geology*, vol. 76, pp. 279–289, 2016.

[9] Q. Luo, S. C. George, Y. Xu, and N. Zhong, "Organic geochemical characteristics of the Mesoproterozoic Hongshuizhuang Formation from northern China: implications for thermal maturity and biological sources," *Organic Geochemistry*, vol. 99, pp. 23–37, 2016.

[10] Q. Luo, Y. Qu, Q. Chen, and Z. Xiong, "Organic geochemistry and petrology of mudrocks from the upper Carboniferous Batamayineishan Formation, Wulungu Area, Junggar Basin, China: implications for petroleum exploration," *Energy & Fuels*, vol. 31, no. 10, pp. 10628–10638, 2017.

[11] L. Wenhao, Z. Zhihuan, L. Youchuan, Z. Gongcheng, and F. Ning, "The development characteristics of source rocks in the main deepwater petroliferous basins of the world and their enlightenment to the study of source rocks in deep- water area of northern South China Sea," *Geology in China*, vol. 41, no. 5, pp. 1673–1681, 2014.

[12] H. Hao, H. Lin, M. Yang, H. Xue, and J. Chen, "The mesozoicin chaoshan depression:A new domain of petroleum exploration," *China Offshore Oil and Gas (GEOLOGY)*, vol. 15, no. 3, pp. 157–163, 2001.

[13] X. Bin, C. Xuejun, X. Jianhua, and W. Ran, "Thinking about the dynamics mechanismstudy on formation and evolution of South China sea," *Geotectonica et Metallogenia,*, vol. 28, no. 3, pp. 221–227, 2004.

[14] K. E. Peters, "Guidelines for evaluating petroleum source rock using programmed pyrolysis," *AAPG Bulletin*, vol. 70, pp. 318–329, 1986.

[15] C. A. Law, "Evaluating source rocks," in *Exploring for Oil and Gas Traps*, E. A. Beaumont and N. H. Foster, Eds., American Association of Petroleum Geologists, Treatise in Petroleum Geology, 1999.

[16] B. Lu, P. Wang, J. Wu, W. Li, W. Wang, and Y. Lang, "Distribution of the Mesozoic in the continental margin basins of the South China Sea and its petroliferous significance," *Petroleum Exploration and Development*, vol. 41, no. 4, pp. 545–552, 2014.

[17] Q. Cai, "Primary hydrocarbon-bearing basins and the pool-forming conditions in China seas and adjacent regions," *Marine Geology & Quaternary Geology*, vol. 18, pp. 1–10, 1998.

[18] H. Hao, X. Zhang, H. You, and R. Wang, "Characteristics and hydrocarbon potential of Mesozoic strata in eastern Pearl River Mouth basin, northern South China Sea," *Journal of Earth Science*, vol. 20, no. 1, pp. 117–123, 2009.

[19] H. Jiaxiong, C. Shenghong, C. Shasha, M. Wenhong, and L. Xiwu, "Early-stage prediction and evaluation of hydrocarbon source rocks in the deepbasin on the northern continental margin of the South China Sea," *Geology in China*, vol. 36, no. 2, pp. 404–416, 2009.

[20] C. Gong, J. Peakall, Y. Wang, M. G. Wells, and J. Xu, "Flow processes and sedimentation in contourite channels on the northwestern South China Sea margin: a joint 3D seismic and oceanographic perspective," *Marine Geology*, vol. 393, pp. 176–193, 2017.

[21] D. Schumacher, "Surface Geochemical Exploration for Petroleum," in *Exploring for Oil and Gas Traps*, E. A. Beaumont and N. H. Foster, Eds., American Association of Petroleum Geologists, Treatise in Petroleum Geology, 1999.

[22] M. A. Abrams, "Significance of hydrocarbon seepage relative to petroleum generation and entrapment," *Marine and Petroleum Geology*, vol. 22, no. 4, pp. 457–477, 2005.

[23] N. R. Cameron and K. White, "Surface Geochemical Exploration Continues to Progress Global Deepwater Frontiers," IBC: Worldwide Deepwater Technologies, London, 2000.

[24] V. T. Jones and R. J. Drozd, "Predictions of oil or gas potential by near-surface geochemistry," *AAPG Bulletin*, vol. 67, no. 6, pp. 932–952, 1983.

[25] W. Li, Z. Zhang, K. Zheng, and Y. Li, "Geochemical characteristics and developmental models of the eocene source rocks in the Qiongdongnan Basin, northern South China Sea," *Energy & Fuels*, vol. 31, no. 12, pp. 13487–13493, 2017.

[26] Q. Luo, N. Zhong, Y. Liu, Y. Qu, and L. Ma, "Organic geochemical characteristics and accumulation of the organic matter in the Jurassic to Cretaceous sediments of the Saihantala Sag, Erlian Basin, China," *Marine and Petroleum Geology*, vol. 92, pp. 855–867, 2018.

[27] W. Zhu, B. Huang, L. Mi, R. W. Wilkins, N. Fu, and X. Xiao, "Geochemistry, origin, and deep-water exploration potential of natural gases in the Pearl River Mouth and Qiongdongnan Basins, South China Sea," *AAPG Bulletin*, vol. 93, no. 6, pp. 741–761, 2009.

[28] C. Jie, "Geophysical characteristics of the Chaoshan depressionand its hydrocarbon exploration potential ," *Progress in Geophysics*, vol. 22, no. 1, pp. 147–155, 2003.

[29] A. D. Hindle, "Petroleum migration pathways and charge concentration: a three-dimensional model," *AAPG Bulletin*, vol. 81, no. 9, pp. 1451–1481, 1997.